

Intensity fluctuations in the Compensated Earth Moon Earth Laser Link (CEMERLL) experiment

B. Martin Levine
Optical Sciences and Applications Section

Kamran Kiasaleh¹
Communications Systems Research Section
Jet Propulsion Laboratory
California Institute of Technology
4800 Oak Grove Drive, M/S 306-388
Pasadena, CA 91109

Abstract

The objectives of the CEMERLL experiment are to measure the signal enhancement obtained in a two way laser propagation link using laser guidestar adaptive optics from the Earth to the Moon using the Apollo retroreflector arrays, and to predict and verify the resulting signal strength and variability. A theory is presented for the probability density functions of the laser link by combining multiple effects of the: 1) compensated laser uplink through turbulence, 2) reflection from the lunar retroreflector array, 3) passage through turbulence on the downlink, aperture averaging by the receiving telescope, and 4) signal detection with a photovoltaic detector. The most important element in the chain is the uplink propagation, all other effects modify only the mean number of photons of this two way link, and do not significantly change the probability density functions of the uplink laser beam.

The resulting probability density functions are defined by parameters that include the effective number of scatterers, the average intensities in the specular and diffuse portions of the beam, and the beam jittering effect of using a laser guidestar. Using intensity moments derived from the far field propagation, performance data on the laser guidestar adaptive optics system, and approximations for higher order moments, the parameters of these distributions can be numerically evaluated from experimental conditions. These show a widely diffuse speckle pattern for the uncompensated beam, and a similar shaped but long tailed distribution for the compensated beam. Uncorrected tilt effects cause the well compensated beam to randomly jitter and results in an intensity distribution where there are some 'hits' of high intensity light, but more frequently there is a portion of the beam side lobes which illuminate the corner cube array. A separate tip-tilt correction using either an illuminated lunar feature or the return pulses themselves would mitigate this effect.

1.0 Introduction

The CEMERLL experiment will be conducted using the facilities of the Starfire Optical Range (SOR), at Kirtland Air Force Base, New Mexico under the direction of JPL [1]. The experiment will measure the return pulses of a ground based laser directed toward an array of retroreflectors on the surface of the moon. CEMERLL will be conducted at two wavelengths, 532 nm and 1064 nm. Adaptive optics is an enabling technology for this experiment. The baseline experiment will measure the signal enhancement obtained by using adaptive optics to concentrate the uplink laser beam thereby increasing the returned signal strength. The second objective of CEMERLL is to verify predictions of signal strength in the two way link.

A schematic of the experiment is given below in Figure 1. An uplink pulsed laser beam is directed from a 1.5 m telescope toward one of a number of corner cube arrays left on the surface of the moon by the Apollo astronauts [2]. The upward beam that has been transmitted through the atmosphere and has propagated to the corner cubes is reflected back to the transmitter site where it is measured using a 3.5 m diameter receiver telescope located 100 meters away. The theory for the CEMERLL laser link developed in this paper is divided by distinct conditions of propagation which are divided by: 1) uplink laser propagation, 2) retroreflected beam, 3) downlink propagation through the atmosphere including aperture averaging, and 4) signal detection.

In Section 2.0, we predict the expected average signal in the experiment in terms of experimental conditions and observable parameters. This average number shows the experiment to be feasible but does not consider the fluctuations expected for the received signal. The remaining sections present a theory for to derive the probability density function (pdf) of photons incident at the receiver telescope as concentrated onto a single point detector for measurement. In Section 3.0 dealing with the uplink, the laser beam accumulates phase fluctuations as it propagates through the atmosphere. It then propagates to the Moon where a portion of the beam is incident on the corner cube array. The number of photons incident on the corner cubes depends on the residual wavefront at the top of the atmosphere which comes from the combination of atmospheric turbulence and phase compensation from the laser guidestar adaptive optics (if any). This uplink beam quality is the most significant factor in this experiment. This section includes the probabilistic model for the effects of atmospheric turbulence and any compensation by adaptive optics on the uplink. Also presented is a correspondence between the observable experimental conditions and parameters of the derived pdf's.

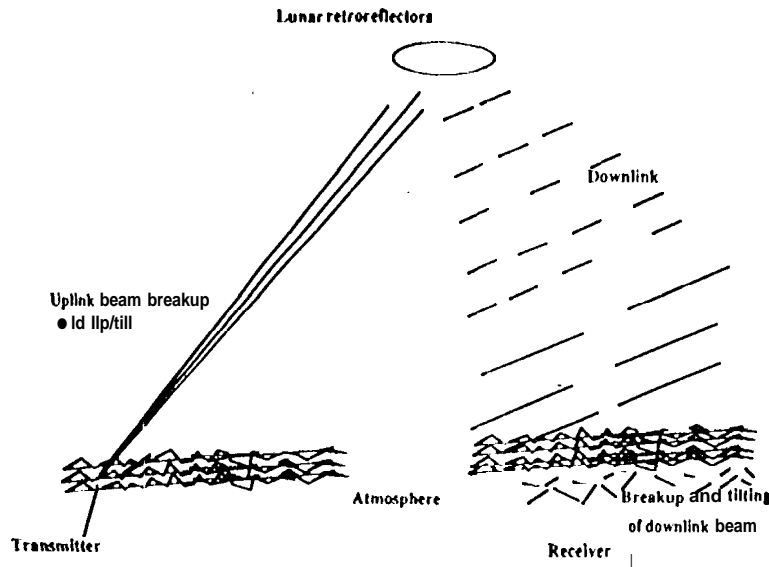
The effect of field summation from the retroreflector array is given in Section 4.0 along with the effect of aperture averaging on the downlink. The effect of the corner cubes will result in an unknown deterministic speckle pattern at the top of the atmosphere on the downlink. We show that aside from reflection and propagation losses, there is no impact on the overall pdf

1. The author is with the Erik Jonsson School of Engineering and Computer Science, the University of Texas at Dallas, P.O. Box 830688, EC33, Richardson, TX 75083. Work was performed while at JPL.

from this component, The return beam passing through the atmosphere will also undergo random phase variations. We will show, in Section 5.0, that this variation is greatly reduced when the receiving aperture is much larger than the size of the atmospheric turbulence cell. That is, the variability of the downlink is insignificant compared to the uplink variability, and aside from propagation losses, there is no impact on the overall pdf. The parameters of these pdf's are predicted by measurements of experimental conditions made during the experiment, namely: the wavelength of the laser beam, the transmitter diameter, range to the moon, bulk transmission losses, the degree of atmospheric turbulence, and the degree of correction by the laser guide star adaptive optics. The pdf moments, e.g., the mean intensity and the mean square intensity provide the mathematical relationships by which the parameters are numerically evaluated from experimental conditions.

Photovoltaic detection of the signal is described in Section 6.0 for the Photomultiplier tube (PMT) detectors, the Solid State Photomultiplier (SSPM), and the Avalanche Photodiode (APD). Incident photons on the detector are converted into photoelectrons to be measured as an electrical signal. The photoelectric signal may be broadened by the detection physics depending on the magnitude of the signal strength. That is broadening will only be significant at the lower signal strengths. Since our expected levels are of the order of 10 or more photoelectrons, this effect is also not significant.

Figure 1: Schematic of the Compensated Earth-Moon-Earth Laser Link (CEMELI) experiment.



2.0 Experimental feasibility

All variables used to predict the mean intensities are either attenuations caused by the optical components such as beam trains and atmospheric transmission or propagation factors such as diffraction on the uplink or propagation on the downlink. Below we give the equations which relate these combinations of factors. A table of numerical values is given in the Appendix Section 8.0.

The uplink intensity on the cornercube is given as the product of factors:

$$\eta_{uplink} = \left(\frac{\lambda p}{hc} \times \tau_{tr} \right) \times \tau_{atm} \left(\frac{\pi D_{tr}^2}{4 (\lambda range)^2} \right) i_{rel} \quad (1)$$

h denotes Planck's constant and c is the speed of light. The first bracketed term is the number of emitted photons in the uplink with a transmission, τ_{tr} , the second term is the due to atmospheric transmission, τ_{atm} . The third term represents the propagation loss by diffraction [3] from a transmitter of diameter, D_{tr} , a wavelength, λ , and a specified range (~ 400 Mm). The last term, i_{rel} , is additional diffraction loss due to turbulence or lack of correction from the adaptive optics, and is equal to unity for a perfect system. The relative number of photons incident on the cornercube is the encircled energy of the beam over the area of the cornercube. The cornercube reflectance is derived using either the cornercube area or the expression for encircled energy within a given area [4] to give:

$$\eta_{retro} = N_{cube} \left(\frac{\pi d_{cube}^2}{4} \right) \times \tau_{cube} \quad (2)$$

where there are N_{cube} cornercubes of diameter, d_{cube} and reflectance, τ_{cube} . On the downlink, the beam propagates geometrically since its divergence angle, θ_{cube} , is greater than the diffraction spread for the cornercube diameter. Thus the transmission factor for the number of photons incident on the receiver telescope as relayed to the detector is the ratio of the areas between the receiver telescope of diameter, D_r , and transmission, τ_r , and the projected cornercube beam multiplied by all the appropriate transmission factors:

$$\eta_{receiver} = \tau_{atm} \times \left(\frac{D_r}{\theta_{cube} range} \right)^2 \times \tau_r. \quad (3)$$

The product of η_{uplink} , η_{retro} , and $\eta_{receiver}$ gives the average number of photons received by the telescope as relayed to the detector. Note that when multiplied together, the two way link contains the range⁴ dependence as expected. The average expected photon return is given in Table 1 below. Although the mean values for the compensated and uncompensated beams are not dramatically different, there are more large magnitude pulses present for the compensated case as will be shown in the following section,

Table 1: Average number of photons expected for CEMERIL phase 1 experiment averaged over nominal conditions.

Condition	$\lambda=532$ run	L-1064 nm	beam quality
uncompensated	12	98	broad speckle pattern of low intensity
compensated	17	155	concentrated beam with atmospheric tilt
compensated + tilt corrected	304	5,240	localized beam; objective for extended experiments
maximum	5,687	12,300	maximum for perfect adaptive optics

3.0 Uplink probability density function

The pdf's for uplink and downlink beams are derived by applying previously published results in laser beam propagation which uses the theory of random walks [5], [6]. The parameters of these pdf's correspond to physical quantities such as the effective number of scatterers, specular and diffuse beam components, and the size of the beam in relation to atmospherically induced tilt.

The effect of atmospheric turbulence on the uplink beam is described in terms of the addition of a large number of statistically independent random complex amplitudes. Following the framework of Strohbeln, Wring, and Speck [5], the atmosphere along the line of sight to the corner cube array is divided into a number, K , of independent slabs, each containing a random magnitude, τ , and phase, ϕ . At the top of the atmosphere, the complex amplitude of the radiation can be characterized as a random phase front which propagates to the corner cube array in the far-field. The on-axis complex amplitude, $a(0,0)$ is effectively given by the summation of magnitude and phase contributions from each of the K atmospheric slabs [6]:

$$a(0,0) = e^{i\omega t} \sum_{k=1}^K \tau_k(0,0) e^{i\phi_k(0,0)}. \quad (4)$$

where $i = \sqrt{-1}$, ω is the optical wave frequency. The probability distributions of τ and ϕ are statistically independent, their functional forms are arbitrary and the only restriction is that the mean phase is taken to be zero (without loss of generality). We also view the uplink as combination of independent specular and diffuse components. The specular component is the part of the beam which suffers few phase perturbations, and the diffuse component is the part of the beam containing greater phase perturbations such as those not correctable by the adaptive optics, e.g. focal anisoplanatism [7], [8]. The symbolic expression is:

$$a(0,0) = a_s(0,0) + a_d(0,0) \\ a(0,0) = \sum_{k=1}^K a_k(\mathbf{o}, \mathbf{o}) e^{i\psi_k(0,0)} + \sum_{k=1}^K a_{dk}(\mathbf{o}, \mathbf{o}) e^{i\phi_k(0,0)} \quad (5)$$

with the resultant intensity being the modulus square of the amplitude:

$$i = |a(0,0)|^2. \quad (6)$$

$a_k(0,0)$ and $\psi_k(0,0)$ are the amplitude and phase of the coherent or specular component of the k th scattered field, respectively, whereas $a_{dk}(0,0)$ and $\phi_k(0,0)$ denote the amplitude and phase of the diffuse random field, respectively. In the analyses to follow, the summation index, K , is replaced by a continuous parameter, α .

3.1 Uncompensated uplink

Historically, log-normal pdf has been employed to characterize the scintillation effects in a turbulence [5]. It is also well-known that the fluctuations drive towards 'saturation' for strong turbulence or when the propagation distance is large, i.e. when the number of scatterers in the turbulent medium is large. The intensity distribution of the optical field is then governed by a negative exponential distribution.

For propagation paths in excess of a kilometer, the validity of log normal and the negative exponential models to accurately model the turbulence-induced scintillation has been challenged for weak and strong turbulence. For small propagation distances, the number of scatterers is typically finite. A number of studies (see [9], [10], [11]) have considered a scattering model with the number of scatterers governed by a negative binomial distribution leading to a K -distributed intensity. This pdf

has also been successfully used to model atmospheric turbulence deep into saturation, but is not readily applicable to weak turbulence.

Andrews and Phillips proposed two universal models for characterizing scintillation [12], [13]. The first model considers the received optical signal as the direct sum of fixed, specular and random, diffuse components. They used a Nakagami distribution (similar to the noncentral Chisquare) to describe the resultant received signal intensity. Given that the diffuse amplitude, a_{diff} , is a Gaussian distributed random variable for an infinite number of random components, Andrews and Phillips derived the I-K distribution by averaging over its modulus square, the diffuse intensity, which becomes (negative) exponentially distributed. The resulting pdf may be used to characterize turbulent optical channels over a wide range of turbulent operating conditions. The intensity moments for this pdf approach unity for very weak turbulence, and goes to $n!$, as predicted by the exponential distribution in the strong turbulence regime. The functional form for this distribution is:

$$p(i_u) = \begin{cases} \frac{2\alpha}{b} \left(\frac{\sqrt{i_u}}{A} \right)^{\alpha-1} K_{\alpha-1} \left(2A \sqrt{\frac{\alpha}{b}} \right) I_{\alpha-1} \left(2\sqrt{\alpha \frac{i_u}{b}} \right) & (i_u < A^2) \\ \frac{2\alpha}{b} \left(\frac{\sqrt{i_u}}{A} \right)^{\alpha-1} I_{\alpha-1} \left(2A \sqrt{\frac{\alpha}{b}} \right) K_{\alpha-1} \left(2\sqrt{\alpha \frac{i_u}{b}} \right) & (i_u > A^2) \end{cases} \quad (7)$$

$K_\alpha(\cdot)$ is the modified Bessel function of the second type and order α , and $I_\alpha(\cdot)$ is the modified Bessel function of the first type of order α . The I-K pdf is specified by three parameters. The term α , is the effective number of scatterers in the uplink, the parameter A^2 , is the average intensity resulting from the specular component, and b is an ensemble average corresponding to the diffuse component of intensity. Since the uplink intensity is a random quantity, due to atmospheric conditions, the overall intensity, i_u , can be either larger or smaller than the average specular component. The n th moment of a random variable is defined as:

$$\langle i_u^n \rangle = \int_0^\infty i_u^n p(i) di \quad (8)$$

and for the I-K distribution is:

$$\langle i_u^n \rangle = \left(\frac{b}{\alpha} \right)^n n! \sum_{k=0}^n \frac{\Gamma(\alpha+n)}{\Gamma(\alpha+k)} \frac{(\alpha\rho)^k}{k!} \quad \rho = \frac{A^2}{b} \quad (9)$$

The first two moments are explicitly written as:

$$\langle i_u \rangle = A^2 + b \quad (10)$$

$$\langle i_u^2 \rangle = A^4 + 2A^2b + 2b^2 + \frac{2}{\alpha} b(b + A^2) \quad (11)$$

The mean intensity can be predicted in advance of the experiment for a laser power, p , along with the other experimental conditions, and is:

$$\langle i_u \rangle = \left(\frac{\lambda p}{hc} \right) \times (\tau_{atm} \tau_{tr}) \times \left(\frac{\frac{\pi D_{tr}^2}{4}}{(\lambda \times range)^2} \right) \times \left(\frac{r_0}{D_{tr}} \right)^2 \quad (12)$$

The last factor is derived from expression for far-field intensity for Kolmogorov turbulence. The second moment is evaluated from (9) in the limit as where $\alpha!$ is large and ρ is small:

$$\langle i_u^2 \rangle = 2 \left(1 + \frac{1}{\alpha} \right) \langle i_u \rangle^2 \quad (13)$$

The parameter α , is computed as the number of coherence areas within the area of the transmitter beam (see the Appendix Section 8.3), and is

$$\alpha = 2.3 \left(\frac{D_{tr}}{r_0} \right)^2 \quad (14)$$

Computed parametric values for the two wavelengths and r_0 of 7 cm are given in Table 2 below. The magnitude of α is so large that A^2 is negligible, and the resultant pdf approaches an exponential pdf. Figure 2 shows predictions of the pdf for expected conditions during CEMERLL using the I-K distribution, and its limiting distributions, the lognormal and the exponential distributions. The I-K tracks very closely with the exponential, but both fall off faster at the larger intensities than the log normal.

3.2 Compensated pdf

In a compensated beam scenario, two important changes are made, in adapting the random walk model to the compensated uplink. These are 1) that the specular component is a random quantity caused by the lack of a tilt correction in the laser guidestar adaptive optics system [7], and 2) the diffuse component is a summation of a small finite number of random components. Because laser guidestar adaptive optics provides progressively less correction at the lower spatial frequencies, the corner cubes will be illuminated by a well corrected but randomly jittered beam. Secondly the effective number of scatterers is

substantially reduced in a compensated beam scenario as compared with an uncompensated case. The Nakagami pdf is independent of the characteristics of the individual scatterers and phase distortions caused by them.

The compensated uplink is modelled in two stages. First we model the pdf of the unjittered beam, and then we combine it with the jitter pdf to obtain the overall model. In the absence of tilt errors, (or conversely for a tilt corrected beam of known tilt error, i_s) the uplink intensity pdf is given by the conditioned pdf which is Nakagami distributed:

$$p(i_c | i_s) = \frac{1}{b} \left(\frac{i_c}{A} \right)^{a-1} \Gamma \left[\alpha \frac{(A^2 i_s + i_c)}{b} \right] I_{\alpha-1} \left(2\alpha \frac{A}{b} \sqrt{i_c i_s} \right) \quad (15)$$

As in the uncompensated case, b denotes the average diffuse intensity and physically represents uncorrected higher order aberrations of the beam. The parameter A is the average specular intensity, i_s is its normalized far field jitter intensity (contained within the interval $[0, 1]$). The fluctuation in the average specular intensity is $A i_s$, where the received optical beam is subjected to atm-sphere-induced pointing tilt, modeled as two dimensional, zero-mean, independent Gaussian random processes with variance σ_j in x and y directions [14]. This tilt or beam jitter term is modeled its a bckr-distributed random variable:

$$p(i_s) = \beta i_s^{\beta-1} \quad 0 \leq i_s \leq 1$$

$$\beta = \frac{\left(\frac{\lambda}{2D_{rr}} \right)^2}{\sigma_j^2} \quad (16)$$

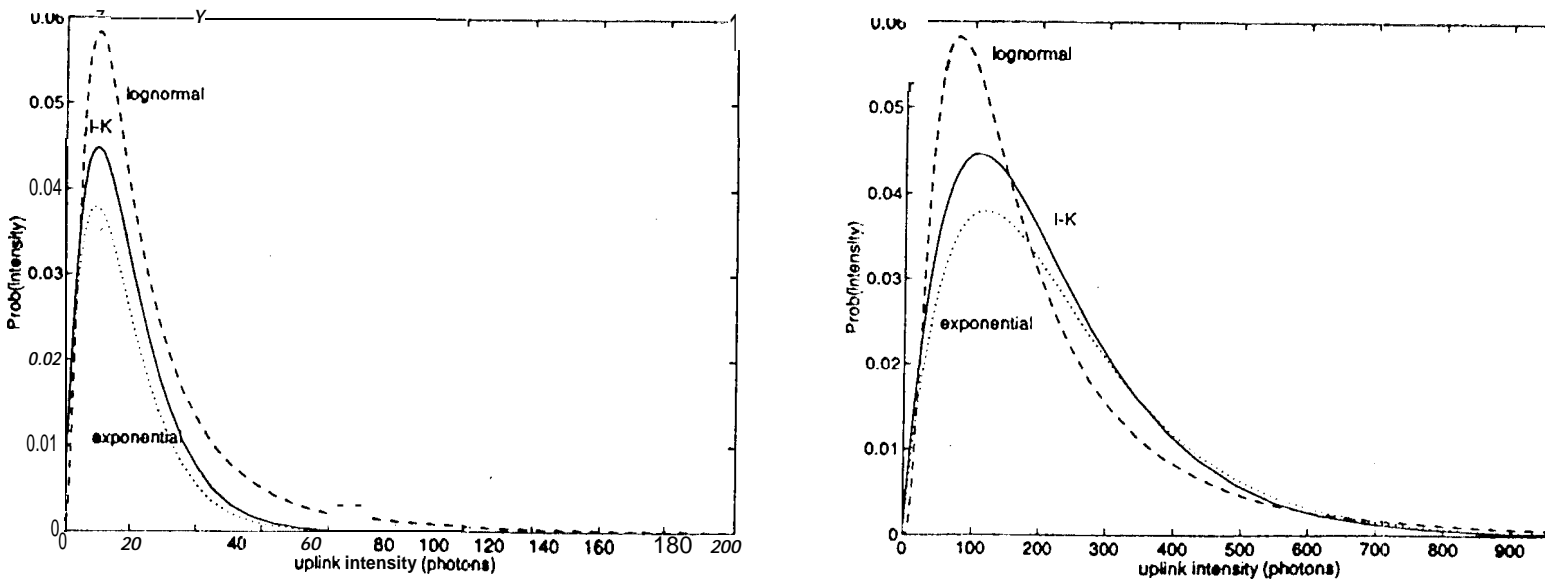
where β is the ratio of the squared beam size to the jitter variance. For adaptive optics corrections on it single mode laser, the full width half max beam size is nearly equal to the diffraction limit. The beam pointing jitter is the mean squared sum of the atmospheric single axis tilt jitter and telescope pointing jitter [15], [16]:

$$\sigma_j^2 = 0.1812 \left(\frac{\lambda}{D_{rr}} \right)^{1/3} \left(\frac{\lambda}{r_0} \right)^{5/3} + (0.6 \mu rad)^2. \quad (17)$$

Table 2: Predicted values of parameters for the uncompensated uplink pdf based on the I-K distribution.

λ	r_0	α	$\langle i_u \rangle$ (photons)	$\langle i_u^2 \rangle / \langle i_u \rangle^2$	A^2 (photons)	b (photons)
532 nm	7 cm	1379	9.5	2.0015	7.1×10^{-12}	9.s
1064 nm	7 cm	261.9	108.2	2.0076	10^{-8}	108.2

Figure 2: Probability density function for an uncompensated uplink beam at 532 nm and 1064 nm with $r_0 = 7$ cm. The solid line is the predicted pdf using the I-K distribution, the dashed line denotes the prediction using the log normal pdf with the same moments, and the dotted line denotes the negative exponential.



Thus, the uplink intensity including the effects of jitter in the laser guide-star compensated beam is given by the integral of the conditional uplink pdf and the jitter pdf:

$$P(i_c) = \int_0^1 P(i_c | i_s) P(i_s) di_s \quad (18)$$

The conditional moments of i_c are given by:

$$\langle (i_c | i_s)^n \rangle = n! \left(\frac{\alpha}{b}\right)^n L_n^{\alpha-1} \left(-\frac{\alpha \Lambda^2 i_s}{b}\right) \quad (19)$$

where $L_n^{\alpha-1}(x)$ is the Laguerre polynomial of order n and index $\alpha-1$. By expanding the Laguerre polynomial and noting that i_s appears only as powers in a series expansion, the moments of i_s are:

$$\langle i_s^n \rangle = \frac{\beta}{n + \beta} \quad (20)$$

which are then substituted in the expressions below. A^* and b are computed from simulations based on performance of the guidestar system [17]. A priori predictions of the mean intensity require the knowledge of the spatial coherence function for the compensated wavefront, which is not readily available. Even so, an expression for the second moment would require the evaluation of a six-fold integral. Instead we evaluate the unconditional and conditional mean intensities, both functions of A^* and b . These ensemble averages are:

$$\begin{aligned} \langle (i_c | i_s) \rangle &= \Lambda^2 i_s + b \\ \langle i_c \rangle &= \Lambda^2 \left(\frac{\beta}{\beta + 1} \right) + b \end{aligned} \quad (21)$$

The given values for theunjittered mean intensity (assuming $i_s=1$) and also the jittered intensity required on the left hand side of (21), A^2 and b are separated to give:

$$\begin{aligned} A^2 &= \frac{\langle (i_c | i_s = 1) \rangle - \langle i_c \rangle}{1 - \beta} \\ b &= \frac{(\langle i_c \rangle - \beta \langle (i_c | i_s = 1) \rangle)}{1 - \beta} \end{aligned} \quad (22)$$

The parameters for this pdf also requires not only the knowledge of some three parameters as in the uncompensated case, i.e., A^* , b , and α , and also requires the knowledge of the parameter, β . An exact evaluation of the parameter, α is not tractable, and requires knowledge of the coherence function of the compensated beam at the top of the atmosphere (see Appendix Section 8.3). Instead α is approximated. An effective r_0 value can be calculated using published values for the performance of the guidestar adaptive optics system. The value for α is also determined by approximation to an equivalent r_0 which is based on the performance of the guidestar adaptive optics system [17]. Table 3 below gives values for the parameters α for both wavelengths for r_0 of 7 cm, their values represent the expected intensity for the two way link, and anticipates the final results showing that the uplink pdf can be measured at the receiver scaled only by propagation losses, and not by any added random variation.

These values are substituted into the parameters, and equation (18) is numerically evaluated to produce the pdf's in Figure 4. The long tail on the 532 nm curve is (here but is not as evident than at the longer wavelength). This is a direct result of the lower performance of the adaptive optics system. The peak of these pdf's are similar in amplitude and location to those of the uncompensated case. The difference is the long tails associated with the higher returns which is responsible for the larger mean intensities. Physically, the compensated beam is much more localized than the uncompensated beam, however, the random jitter effectively jitters the beam and reduces the irradiance onto the corner cube array except when the beam excursion is small.

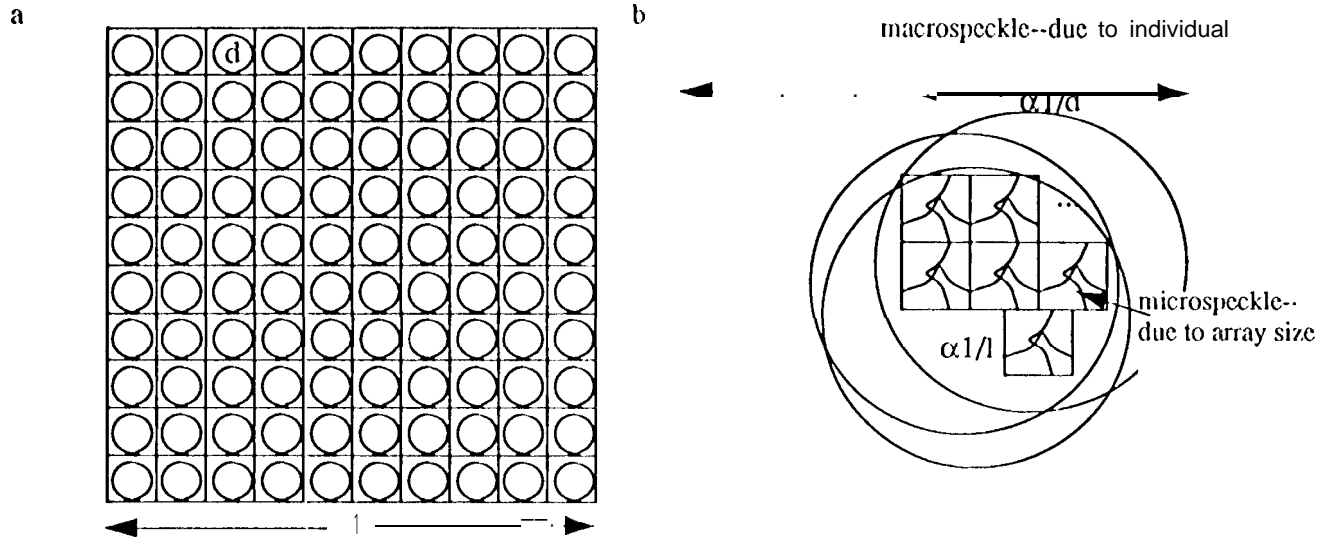
4.0 The retroreflected beam

The targeted circular corner cubes are embedded in a rectangular array (Figure 3a). Within its acceptance angle [19], [20], each of the corner cubes reflects a portion of the incident plane wave back along the direction of the propagation to its source point. Neither is it assumed nor is it known if the phase delays of the individual corner cubes are related in any way. We assume that the offset in phase between each corner cube is most likely greater than 2π . The retroreflected beam is thus described as a sum of quasi-monochromatic sources radiating within the envelope of the corner cube may. The return beam is the interference between each of the individual corner cubes resulting in a fixed but unknown speckle pattern at the top of the atmosphere (in the far field). The speckle pattern is characterized by a 'macro' speckle pattern due to the shape of the individual corner reflectors. Superimposed on this is a 'micro' speckle pattern due to the envelope of the corner cube array (Figure 3b). The combined effect of these two shapes is to produce an overall speckle pattern characterized by a coherence area. For a uniformly bright source, the coherence area for any wavelength, λ , and propagation distance, z , is proportional to the area of the source, A_{source} , given by the simplifying equation [6]:

$$A_c = \frac{(\lambda z)^2}{A_{source}} \quad (23)$$

The coherence diameter is approximately the square root of these quantities, 607 m and 1214 m for the green and infrared wavelengths, respectively. Because the correlation distance of the downlink beam at the top of the atmosphere is so large, subsequent beam breakup on the downlink through the atmosphere can be described in terms of the interference between spatially coherent propagating light waves.

Figure 3: a) Corner cube arrangement for the 10 x 10 Apollo 11 corner cube array of cubes with diameter, d arranged on a grid with dimension, 1. b) Propagation from the corner cube array to the top of the atmosphere results in a fixed but unknown speckle pattern of intensity consisting of a micro-speckle pattern within an envelope of a macro-speckle pattern. The transverse distance of a micro speckle is roughly proportional to the coherence area.



5.0 Downlink atmospheric turbulence and aperture averaging

5.1 Downlink atmospheric turbulence

Because atmospheric turbulence breaks up the phase front of the 'micro' speckle patch as it propagates through the atmosphere, the interaction of the retroreflected laser beam with atmospheric turbulence is described in terms of the addition of a large number of statistically independent random complex amplitudes. The beam propagation calculation uses the same arguments and analysis for the uncompensated uplink described in Section 3.1. Equation (4) is rewritten for the downlink as the complex sum of real and imaginary parts over all spatial coordinates:

$$A(x, y) = \sum_{k=1}^N A_{rk}(x, y) + i \sum_{k=1}^K A_{ik}(x, y) \quad (24)$$

For good atmospheric conditions, this random sum will yield in a log normal pdf for intensity, and for saturated conditions of turbulence, it will yield the (negative) exponential pdf [6]:

$$p(I(x, y)) = \frac{1}{\langle I(x, y) \rangle} e^{-I(x, y) / \langle I(x, y) \rangle} \quad (25)$$

The parameter, $\langle I(x, y) \rangle$, is the mean (ensemble average) of the instantaneous intensity.

5.2 Aperture averaging of the received intensity

The total measured energy per laser beam pulse is the integral of the instantaneous intensity over the entrance pupil, i.e.

$$E = \iint I(\mathbf{r}, y) dx dy \quad (26)$$

The pdf of the integrated energy is determined from its point statistics by recasting the problem as one where the integration is replaced by a summation [6]:

$$E \approx \Delta x \Delta y \sum_j \sum_k I(x_j, y_k) = \frac{A}{N} \sum_{j=1}^J \sum_{k=1}^K I(x_j, y_k) \quad (27)$$

over a number, $N=J * K$, of equal areas over the receiver area, A. Each subarea is characterized as having an exponential pdf for its intensity fluctuations, equation (25), with the same mean, $\langle I_A \rangle$. The mean energy is given by the expression:

$$\langle E \rangle = A \langle I_A \rangle \quad (28)$$

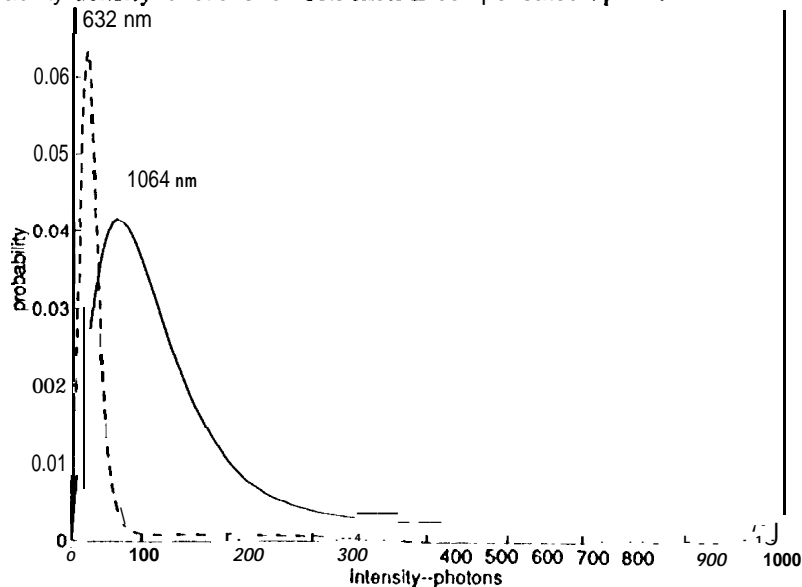
The ensemble average $\langle E \rangle$ is the total integrated intensity over the entire aperture. Using equation (27), the variance of the aperture averaged intensity is related to the variance of a single turbulence cell by the factor of $1/N$:

$$\sigma^2_E = \frac{A^2 \sigma^2_I}{N} \tag{29}$$

Table 3: Parametric values for CEMERILL compensated uplink for $r_0=7$ cm. The values of AZ and b also include transmission and diffraction losses in the downlink.

wavelength	effective r_0	jittered intensity $\langle i_i \rangle$ (photons)	lilt corrected intensity $\langle i_i i_i = 1 \rangle$ (photons)	α	β	A^2 (photons)	b (photons)
532 nm	1.67 m	21	464	2.363	0.00621	446.3	17.7
1064 nm	3.84 m	214	6505	1.270	0.02498	6451	54

Figure 4: Predicted probability density functions for CEMERILL compensated uplink.



As in the uncompensated uplink, the number of subareas, N , is determined by computing the correlation area of the atmospheric turbulence and dividing that number into the receiver area. The number of effective independent contributions is then given by (14), and for the 3.5m receiving aperture and the nominal conditions given for r_0 , its value is over 1400! For large amount of aperture averaging, and one would suspect the pdf of the resultant integrated intensity would converge to that of a Gaussian or other narrow width limiting distribution. For the exponential where the exact integrated intensity pdf goes as a Chi-square distribution with $2N$ degrees of freedom with moments:

$$\langle E^k \rangle = \frac{\Gamma(k + N) \langle E \rangle^k}{\Gamma(N)} \tag{30}$$

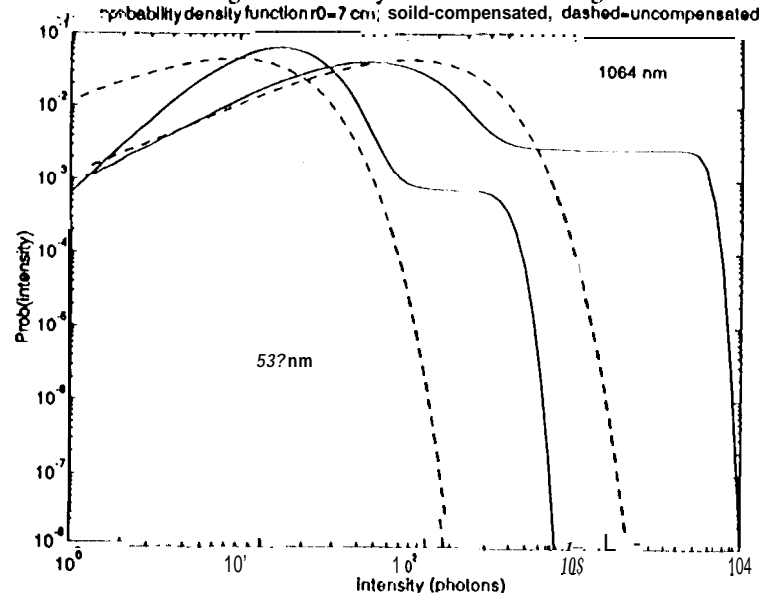
Using this formula, the variance of the aperture averaged intensity is:

$$\sigma^2_E = \langle E^2 \rangle - \langle E \rangle^2 = \frac{\langle E \rangle^2}{N} \tag{31}$$

and the, above pdf converges to a Gaussian with mean and variance as given.

From either (29) and (31), the ratio of standard deviation to the mean intensity for the aperture averaged signal is proportional to $\frac{1}{\sqrt{N}}$. It is less than 3 percent than that of the uplink. Thus the measurement of the downlink is 'noiseless' relative to the fluctuation in the uplink, and does not contribute to the probability density function of the overall two way link. That is, the Gaussian pdf for the downlink acts as if it were a Dirac delta function on the uplink pdf resulting in an overall pdf that follows the functional form of the uplink pdf but whose mean and higher moments are modulated by propagation losses. The numerical value of the mean intensity in the two way link pdf is determined by the experimental conditions and computed by the scaling equations given in Section 2.0. The overall compensated and uncompensated pdf's are summarized below in Figure 5.

Figure 5: Two way link probability density functions for CEMERLL for atmospheric conditions of $r_0 = 7$ cm are used. A log-log scale is used to include the ranges of intensity from both wavelengths.



6.0 Signal detection

The output from in two way laser link will be an electrical current proportional to the number of the generated primary photoelectrons, n_p , and detector gain, G , to give a number of secondary photoelectrons [21]:

$$n_s = G \times (n_p + n_{back}) \tag{32}$$

The second term corresponds to the number of background electrons which is typically due to dark noise but can also be due to noise sources associated with the detector electronics. We assume the number and probability of primary electrons due to the backgrounds observable, and hence, can be deconvolved from the observed signal to obtain an estimate of the true signal. Photovoltaic detectors such as photomultiplier tubes (PMT), avalanche photodiodes (API), and the Solid State Photomultiplier (SSPM) [22], emit a stream of primary photoelectrons generated at random according to a Poisson probability law [6]. The parameter of the Poisson distribution is proportional to the number of photons incident on the detector and its quantum efficiency. Thus the probability of generating n_p photoelectrons obeys Mandel's equation (also known as the Poisson transform) to give a pdf with associated parameter:

$$p(n_p) = \int_0^\infty \frac{W^{n_p} e^{-W}}{n_p!} p(W) dW \tag{33}$$

$$W = \eta E \tag{34}$$

The quantum efficiency of the detector is denoted by, η .

The signal due to these primary photoelectrons is further multiplied by the gain of the detector. The physical mechanism that produces this gain also produces a random variability in the gain which further produces a variation on the number of secondary photoelectrons. PMT technology has been sufficiently developed to produce devices with negligible gain variation [23], and measurements on the SSPM shows the ability for linear recording of multiple photon events [22]. Only the APD technology shows a broadening, of the number of secondary electrons due to gain variability [24]. The variability is a function of the gain, and parameter, k , which governs the noise properties of the APD to give a pdf for secondary electrons, n_s , as function of a constant input of primary photoelectrons, n_p .

$$p(n_p, n_s = n_p + r; G) = \frac{n_p (1-k)^r \Gamma\left(\frac{n_p + r}{1-k}\right)}{(n_p + kr) r! \Gamma\left(\frac{n_p + kr}{1-k}\right)} \left(\frac{1+k(G-1)}{G}\right)^{\frac{(n_p + kr)}{(1-k)}} \left(\frac{G-1}{G}\right)^r \tag{35}$$

This pdf combines with the pdf of the primary photoelectrons to give the overall pdf of secondary photoelectrons in the summation:

$$p(n_s) = \sum_p p(n_p, n_s; G) \times p(n_p) \tag{36}$$

Using the pdf for the two way link using a compensated uplink, the number of primary photoelectrons from equation (33) is evaluated by using the conditional uplink pdf defined in (15) to find the conditional pdf, $p(n_i)$ which is:

$$p(n_c | i_s) = \frac{\mu^c}{(1+\mu)^{c+\alpha}} e^{-\frac{\mu i_s}{1+\mu}} \left(\frac{\mu i_s}{\mu(1+\mu)} \right)^\alpha \quad \mu = \frac{b}{a} \quad (37)$$

The unconditional pdf is obtained by integrating over all probabilities of the jitter pdf as was defined in equation (16). For the case of a two way link using an uncompensated uplink, we compare $p(n_u)$ computed from the exponential pdf (25), which from Figure 2 is a limiting form of the I-K pdf. This results in the Bose Einstein pdf, $p(n_u)$ for primary photoelectrons:

$$p(n_u) = \frac{(W)^{n_u}}{(1+(W))^{1+n_u}} \quad (38)$$

The values for η equal to 8070 for the visible and 870 for the infrared (characteristics of the most APD and SSPM at these respective wavelengths). The APD gain and parameter, k , is assumed from the type of device used [25].

A comparison of the cumulative density (cdf) for secondary photoelectrons, $p(n_s)$, is made against the cdf's of primary photoelectrons, $p(n_p)$, scaled by a uniform gain, and $p(W)$, the detector photon intensity scaled by the quantum efficiency and gain. For our purposes, the cdf is defined:

$$cdf(x) = p(x > x) \quad (39)$$

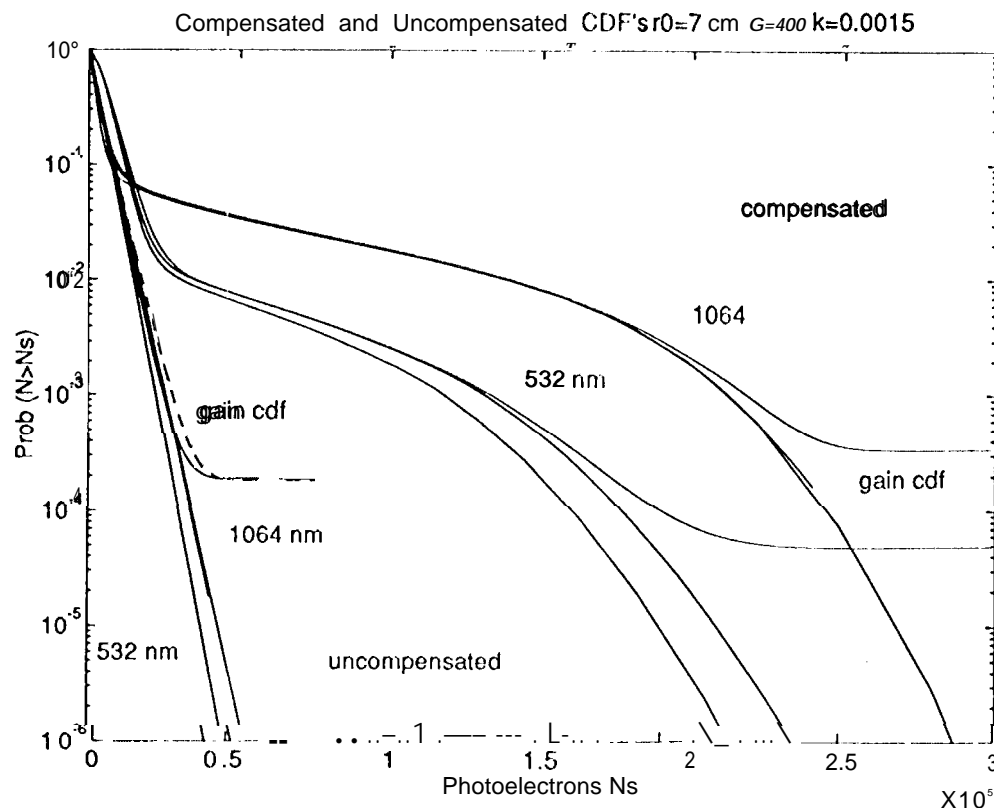
These are all shown in Figure 6 for both compensated and uncompensated cases. We compare cdf's instead of pdf's here because the photoelectron distribution is discrete whereas the photon count pdf, $p(W)$, is inherently a continuous function. So instead of integrating the photon count pdf over discrete intervals, it is easier to compare the two on the cdf. There is some broadening for the high primary photoelectron count levels at both wavelengths but in general the differences are small. The tails of the cdf's for the secondary photoelectrons are all uniformly larger due to the gain variability in APD detector, but are not significant at the probability levels likely to be encountered in CEMERILL.

7.0 Summary

A theory for establishing the probability density functions for the two way laser link in CEMERILL have been presented, and have been numerically evaluated over a range of expected experimental conditions. The two way link pdf's combined the effects of: 1) uplink turbulence, both for the compensated and uncompensated cases, 2) interaction with the corner cubes, 3) downlink propagation through turbulence, averaging effects from a large diameter receiver aperture, and 4) photovoltaic detection effects. The uplink pdf is the most critical factor in determining the two way link pdf. The other effects served to scale the expected number of received photons without appreciably changing the functional form of the probability distribution. A small amount of broadening in the photoelectron counting cdf is also observed using a PMT or SSPM. Broadening due to an APD detector will affect the tails of the secondary electron pdf's in a small way.

The difference between the compensated and uncompensated beam pdf's is the long tails caused by large uplink intensities which recur at random due to the jittering effects from the lack of a tilt error signal. A separate tip-tilt correction would mitigate this effect making for a large return beam for each pulse. Such a system could use a distinct solar illuminated feature on the lunar surface within the isoplanatic patch of the adaptive optics system, or could be initiated by one of these large return pulses.

Figure 6: Comparison of cumulative density functions in CEMERILL.



Acknowledgments

The authors would like to acknowledge of Brent Ellerbrock, US Air Force Phillips Laboratory, and Keith Wilson, Michael Shao, Jim Lesh, and Tsun-Yee Yan of JPL for their help in guiding and reviewing this work. The research described in this paper was carried out at the Jet Propulsion Laboratory, California Institute of Technology under contract with the National Aeronautics and Space Administration.

8.0 Appendix

8.1 Experimental conditions

A common set of parameters governing the atmosphere and the corner cube array all have either been directly measured during GOPEX or have been calculated from other quantities measured at that time. These numerical values have been summarized in Table 4 below. Unless otherwise stated in the table, the experimental quantities vary approximately by +/- 10%.

The turbulence to be corrected decreases due to the wavelength dependence on r , by over a factor of 2 (the ratio of the two wavelengths to the 6/5 power). There is also slightly less transmission loss in the IR than in the visible. Thus the IR photon flux incident on the retroreflector would be greater in both the compensated and the uncompensated uplinks.

Factors for the performance of the laser guide star adaptive optics system were inferred from performance data supplied by SOR [18]. Laser guide star adaptive optics does not provide a signal to correct the effect attributed to tilt in the aperture, and performance values for tilt corrected compensation is included as reference in the given pdf analysis.

The baseline corner cube arrays are the ones left on the Moon by the 3 Apollo missions. The Apollo 11 and Apollo 14 arrays are optically identical, a 10 x 10 array of 3.8 cm diameter cubes arranged on 4.6 cm centers [19]. The Apollo 15 array consists of 300 corner cubes in a close packed hexagonal cell format arranged in a 61 cm x 104 cm rectangle [20]. Each corner cube provides a return beam equivalent to 42 urad divergence angle in both the lunar day and night environment. Total internal reflection is used as the reflecting mechanism instead of metallic coatings (such as aluminum), thus the reflection efficiency is limited to a maximum of 25%.

Table 4: Expected atmospheric and experimental conditions for CEMERIL.

	properly	symbol	$\lambda =$ 532 nm	$\lambda =$ 1064 nm
Atmospheric parameters	maximum zenith pointing angle (degrees)	zenith	45	45
	zenith atmospheric transmission	τ_{zen}	0.8	0.8
	transmission loss (magnitude/ air mass)	m_v	0.2	0.1
	scaled transmission at 45 degrees $\tau_{atm} = \tau_{zen} 10^{-0.4 m_v \sec(\text{zenith})}$	τ_{atm}	0.62	0.70
	$r = 5$ cm minimum atmospheric turbulence at 0.5 μm and zenith pointing scaled to wavelength and maximum zenith pointing angle	r	4.38	10.05
	$r_0 = 6.38$ cm nominal atmospheric turbulence at 0.5 μm and zenith pointing (expected range is 5-7 cm) scaled to wavelength and maximum zenith pointing angle	r	5.58	12.83
	$r = 7$ cm maximum atmospheric turbulence at 0.5 μm and zenith pointing scaled to wavelength and maximum zenith pointing angle	r	6.13	14.07
Telescope transmitter	diameter (m)	D_{tr}	1.5	
	transmission (tip/tilt tracking mode)	τ_{tr}	0.45 (0.25)	
	pulse energy (joule)	p	0.45	1.5
	pulse length (nsec)	t_p	15	15
	repetition rate (Hz)	f	20	20

Table 4: Expected atmospheric and experimental conditions for CEMERLL

	property	symbol	$\lambda = 532 \text{ nm}$	$\lambda = 1064 \text{ nm}$
uplink propagation factor	uncompensated at max r.	i_{rel}	0.0024	0.0100
	laser guidestar compensation at max r.	i_{rel}	0.0036	0.0174
	laser guidestar + tip/tilt compensation at nominal	i_{rel}	0.0863	0.5289
	laser guidestar compensation averaged over r. range	i_{rel}	0.0029	0.0130
Receiver telescope	diameter (m)	D_r	3.5	
	transmission	τ_r	0.5	
Corner cube parameters	cube diameter (cm)	d_{cube}	3.8	
	divergence angle (μrad)	θ_{cube}	42	
	reflection efficiency	τ_{cube}	0.245	
	number of elements--Apollo 11, Apollo 14 (used in report). (Apollo 15)	N_{cube}	100 (300)	

8.2 Far field intensity for propagation through atmospheric turbulence

The complex amplitude in the far field is related to the complex amplitude of the source through the Fraunhofer diffraction integral. Ignoring unimportant complex phase factors, for an amplitude a_0 , and a wavelength, λ , this relation is:

$$a(x, y) = \frac{ia_0}{\lambda z} \iint_D a(\xi, \eta) e^{-i2\pi(u\xi + v\eta)} d\xi d\eta \tag{40}$$

The intensity is the modulus square of this result. In the case of diffraction limited propagation, the function $a(\xi, \eta)$ is a circular aperture, the intensity becomes [3]:

$$I(x, y) = I_0 \left(\frac{\pi D^2}{4\lambda z} \right)^2 \left[\frac{2J_1 \left(\frac{\pi D r}{\lambda z} \right)}{\frac{\pi D r}{\lambda z}} \right]^2 r = \sqrt{x^2 + y^2} \tag{41}$$

The propagation distance is so long that the corner cube array on the moon is at the (0,0) coordinate. Thus the diffraction limited intensity is simply the scale value in front of the Bessel function.

Because of atmospheric turbulence, the value of $a(\xi, \eta)$ represents an instantaneous amplitude, and is a random function. The Fourier kernel drops out of (40) for the on axis far field intensity, and the result is a four fold integral. The ensemble average for this intensity is:

$$\langle I(0, 0) \rangle = \frac{ia_0}{\lambda z} \iint_D \iint_D \langle a(\xi, \eta) a^*(\xi', \eta') \rangle d\xi d\eta d\xi' d\eta' \tag{42}$$

By definition, the spatial coherence function [3] is the bracketed term on the right hand side of the equation, thus:

$$\langle I(0, 0) \rangle = \frac{I_0}{(\lambda z)^2} \iint_D \iint_D \mu(\xi, \eta; \xi', \eta') d\xi d\eta d\xi' d\eta' \tag{43}$$

For uncompensated atmospheric turbulence, the spatial coherence function is given by (53), and is parametrized by Fried's parameter, r_0 [7], [16]:

$$\langle I(0, 0) \rangle = \frac{I_0}{(\lambda z)^2} \iint_D \iint_D e^{-\frac{r^2 + r'^2 + (\eta - \eta')^2}{r_0^2}} d\xi d\eta d\xi' d\eta' \tag{44}$$

These variables of integration are transformed into a difference coordinate with unit Jacobian making the integral a function of the difference alone which can be integrated to reduce the expression to a double integral. Finally, the integral can be transformed into polar coordinates to give a compact form that can be transformed into a Gamma function [27], and by realizing the condition that r_0 is much smaller than the telescope aperture.

$$I(\mathbf{o}, \mathbf{o}) = \frac{I_0 \left(\pi \frac{D^2}{4} \right) \left(\frac{\pi r_0^2}{4} \right)}{(\lambda z)^2} \quad \text{for } D \gg r_0 \quad (45)$$

This value is compared to the diffraction limited intensity in (41) to give the relative intensity:

$$i_{urb} = \left(\frac{r_0}{D} \right)^2 \quad (46)$$

which is the factor given to compute the mean intensity for the uplink in Section 3.1, equation (12).

8.3 Coherence area and the effective number of scatterers.

The number of effective scatterers in the uplink is the ratio of the transmitter area to the coherence area of the uplink beam with the coherence area defined as:

$$A_c \approx \int_{-\infty}^{\infty} \int_{-\infty}^{\infty} |\mu(\Delta x, \Delta y)|^2 d\Delta x d\Delta y \quad (47)$$

This integration is identical to that of the mean far field intensity as shown above, except for the square of the coherence function and that polar coordinates are used on a double integral at the beginning. For Kolmogorov turbulence, the required integration can be performed in closed form in a way similar to the previous section to give the final result:

$$\alpha = \frac{n D^2}{A_c} = 2.3 \left(\frac{D}{r_0} \right)^2 \quad (48)$$

For the compensated case, the limiting approximation does not hold and the solution to (47) involves an incomplete gamma function which we numerically evaluate for this paper. The numerical integral requires the use of an effective value of r_0 , which is taken from the reported seeing angle, θ , measured by the laser guide star adaptive optics system [17].

$$r_{0eq} = \frac{\lambda}{\pi \theta} \quad (49)$$

For 0.13 arcsecond seeing at $\lambda_0 = 0.88 \mu\text{m}$ [18], the effective r_0 is scaled to the CEMERILL wavelengths and zenith angle, ϕ , through the scaling equation:

$$r_{0eff} = r_{0eq} \left(\frac{\lambda}{\lambda_0} \right)^{6/5} \cos^{-3/5} \phi \quad (50)$$

9.0 References

1. K. H. Wilson, 'Overview of the Compensated Earth-Moon-Earth Retroreflector Laser Link (CEMERILL) experiment', SPIE v2123-07, 1994.
2. P.L. Bender, et. al., "The Lunar laser ranging experiment", Science, v182, p229-238, (1973).
3. J. Goodman, Introduction to Fourier Optics, McGraw Hill, New York, Equation 4-17, p64, 1968.
4. Born and E. Wolf, Principles of Optics, fifth edition, Pergamon Press, New York, Equation 18, p398, 1975.
5. J.W. Strohbehn, T. Wang, and J.P. Speck, "On the probability distribution of line-of-sight Fluctuations of optical signals", Radio Science, v10, 59-70, 1975
6. J. Goodman, Statistical Optics, J. Wiley and Sons, New York, 1985, Section 5, p180 and p210. See also Appendix B and pages 31-33 for the discussion of Gaussian distributed complex amplitudes, and Section 6.1.2 for the derivation of integrated intensity. Sections 2.5.3 and 2.9.3 show how the exponential intensity is derived from joint Gaussian distributed pdf's. Section 9 discusses the basis of photoelectric detection.
7. R.Q. Fugate, 'Laser guide star adaptive optics for compensated imaging', Section 1.7 of The Infrared and Electro-optical Systems Handbook, Volume 8, Emerging Systems and Technologies, Stanley R. Robinson, Editor, SPIE press, Bellingham, WA, 1993.
8. R.Q. Fugate, D.L. Fried, G.A. Ammer, B.R. Boeke, S.L. Browne, P.H. Roberts, R.E. Ruane, and L.M. Wopat, "Measurement of atmospheric wavefront distortion using scattered light from a laser guide star", Nature, 353, 144-146, 1991.
9. R. Barakat, "Weak-scatterer generalization of the K-density function with application to laser scattering in atmospheric turbulence. J. Optical. Soc. Amer. A, 3, pp401-409, 1986.
10. R. Barakat, "Weak-scatterer generalization of the K-density function. 11. Probability density of the total phase.", J. Optical. Soc. Amer. A, 4, pp1213-1219, 1987.

11. R. Barakat, "Direct deviation of intensity and phase statistics of speckle produced by a weak scatterer from the random sinusoid model", *J. Optical. Soc. Amer.*, 71, pp86-90, 1981.
12. R.L. Phillips and L.C. Andrews, "Universal statistical model for irradiance fluctuations in a turbulent medium", *J. Optical. Soc. Amer.*, 72, pp160-163, 1985.
13. L. C. Andrews and R. L. Phillips, "I-K distribution as a universal propagation model of laser beams in atmospheric turbulence", *J. Optical. Soc. Amer. A*, 2, pp401-409, 1986.
14. K. Kiasaleh and T.-Y. Yan, "A statistical model for evaluating GOPEX uplink performance", TDA progress report 42-111, Jet Propulsion Laboratory, November 1992.
15. R.J. Nell, "Zernike polynomials and atmospheric turbulence", *J. Optical. Soc. Amer.*, 76, pp207-211, 1976.
16. F. Roddier, "The effects of atmospheric turbulence in optical astronomy", Progress in Optics, XIX, E. Wolf, ed. North-Holland, New York, 1980. See Section 7.5.
17. R.Q. Fugate et.al., "two generation of laser guide star adaptive optics experiments at the Starfire Optical Range", accepted for publication in the *J. Optical. Soc. Amer. A*, feature issue on Atmospheric Compensation Technology, 1993.
18. R.Q. Fugate, "GOPEX at the Starfire Optical Range", JPL "TDA Progress Report 42-114, pp255-279, August 15, 1993.
19. R. F. Chang, C.O. Alley, D.G. Currie, and J.E. Faller, "Optical properties of the Apollo laser ranging retroreflector 'arrays'", *Space Research*, vol. XII, p247-259, 1972.
20. J.E. Faller, "The Apollo retroreflector arrays and a new multi-lensed receiver telescope", *Space Research*, v XII, p 235-246, 1972.
21. S. Karp, R.M. Gagliardi, S.E. Moran, and L.B. Stotts, Optical Channels, Plenum Press, New York, 1988, Section 3.5.
22. P.G. Kwiat, A.M. Steinberg, R.Y. Chiao, P.H. Eberhard, and M.D. Petroff, 'High-efficiency single-photon detectors', *Phys. Rev. A*, v48, R867-R870, 1993.
23. G.F. Knoll, Radiation Detection and Measurement, second edition, J. Wiley and sons, New York, 1989, p259. Also see the RCA Photomultiplier Handbook, publication PMT-62, 1980, p158-160.
24. R.J. McIntyre, 'The distribution of gains in uniformly multiplying avalanche photodiodes: theory', *IEEE Trans. on Elect. Devices*, ED-19, 703-712, 1972.
25. 'Tim Avalanche photodiode catalog', Advanced Photonix, Inc. Camarillo, CA.
26. B.M. Levine, "Data analysis for GOPEX image frames", TDA Progress Report 42-114, pp213-229, August 15, 1993.
27. M. Abramowitz and I.A. Stegun, eds., Handbook of Mathematical Functions, Dover, New York, 1972, p255.

Intensity fluctuations in the Compensated Earth Moon Earth Laser Link (CEMERLL) experiment

B. Martin Levine

Jet Propulsion Laboratory

California Institute of Technology

Pasadena, CA 91109

and

Kamran Kiasaleh

University of Texas at Dallas

Richardson, TX 75083

CEMERLL Intensity fluctuations

Overview:

- experimental **objectives and applications**
- **critical paths and components in propagation**
- **development of theory**

feasibility (expected photon returns)

intensity pdf's and associated parameters

relationship between parameters and expected returns

probability density function (pdf) predictions

CEMERLL Intensity fluctuations

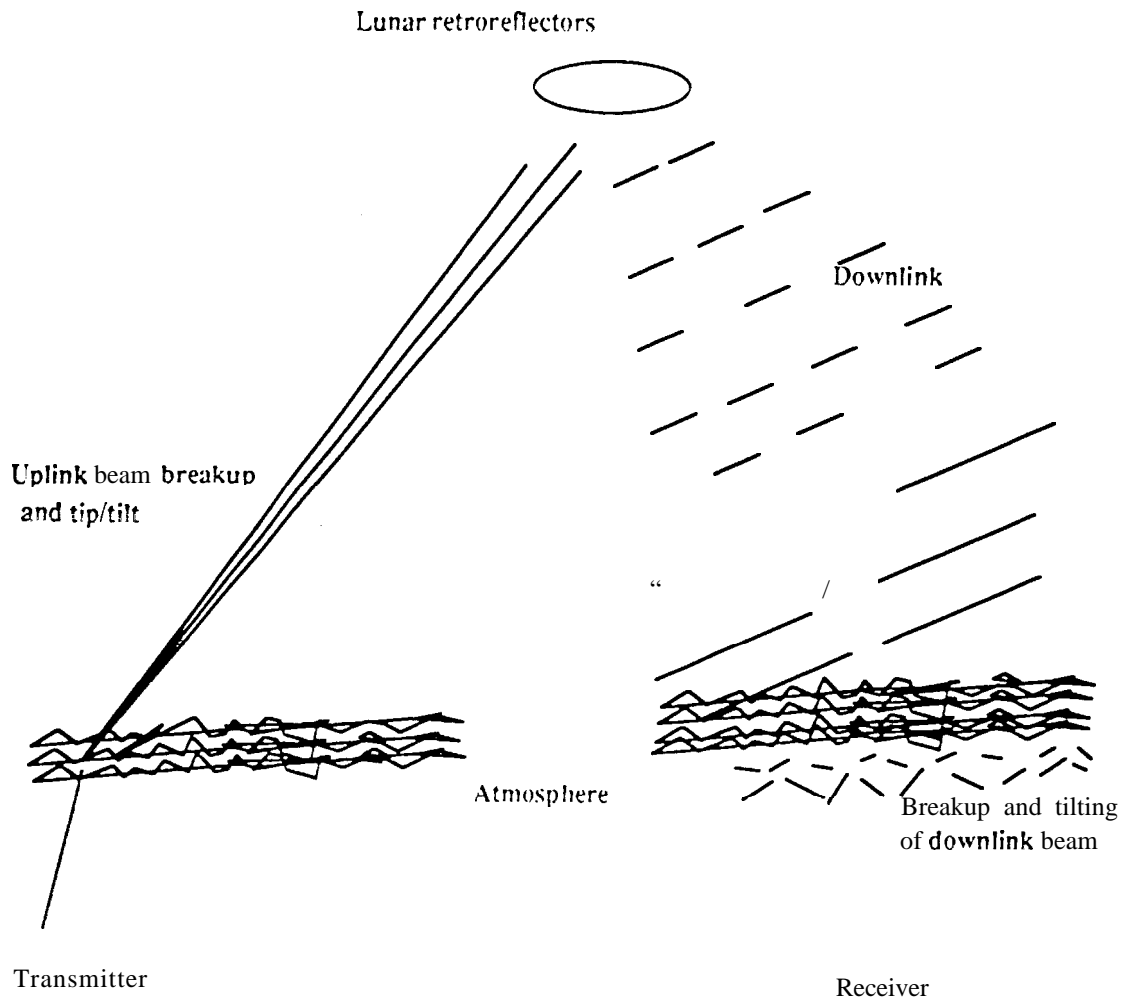
Objectives:

- **To measure signal enhancement in a two way laser propagation Link
between Earth and Moon
with'without laser guidestar adaptive optics at Starfire Optical Range
at 532 nm 1064 nm wavelengths**
- **Testbed for deep space optical communications Links
precision pointing and tracking
low power laser propagation statistics through atmospheric turbulence**

CEMERLL Intensity fluctuations

Critical propagation paths and components:

- Uplink
- Corner cubes
- Downlink
- propagation turbulence
- aperture averaging
- Detection



CEMERLL Intensity fluctuations

Theory development

- **Feasibility (Expected returns)**

 - point analysis based on a priori experimental conditions**

- **Intensity pdf's**

 - parameterized probability density functions**

- **Relationship between pdf parameters and point analysis**

- **Result is a theory which gives the functional form of the pdf's for-received intensity and the relationship between its parameters and the experimental conditions**

CEMERLL Intensity fluctuations

Feasibility study:

Expected atmospheric and experimental conditions for CEMERLL

	property	symbol	$\lambda=532$ n m	$\lambda=1064$ nm
Atmospheric parameters	maximum zenith pointing angle (degrees)	zenith	45	45
	zenith atmospheric transmission	τ_{zen}	0.8	0.8
	transmission loss (magnitude/ air mass)	m_v	0.2	0.1
	scaled transmission at 45 degrees $\tau_{atm} = \tau_{zen} 10^{-0.4 m_v \sec(\text{zenith})}$	τ_{atm}	0.62	0.70
	r. =5 cm minimum atmospheric turbulence at 0.5 μ m and zenith pointing scaled to wavelength and maximum zenith pointing angle	r.	4.38	10.05
	r0 = 6.35 cm nominal atmospheric turbulence at 0.5 μ m and zenith pointing (expected range is 5-7 cm) scaled to wavelength and maximum zenith pointing angle	r0	5.58	12.53
r. =7 cm maximum atmospheric turbulence at 0.5 μ m and zenith pointing scaled to wavelength and maximum zenith pointing angle	r0	6.13	14.07	
Telescope transmitter	diameter (m)	d_{tr}	1.5	
	transmission (tip/tilt tracking mode)	τ_{tr}	0.45 (0.25)	
	pulse energy (joule)	p	0.45	1.5
	pulse length (nsec)	t_p	15	15
	repetition rate (Hz)	f	20	20

CEMERLL Intensity fluctuations

Expected atmospheric and experimental conditions for CEMERLL

	property	symbol	$\lambda=532$ n m	$\lambda=1064$ nm
uplink propagation factors'	uncompensated at max r.	i_{rel}	0.0024	0.0100
	laser guidestar compensation at max r.	i_{rel}	0.0036	0.0174
	laser guidestar + tip/tilt compensation at nominal	i_{rel}	0.0S63	0.52S9
	laser guidestar compensation at averaged over r. range	i_{rel}	0.0029	0.0130
Receiver telescope	diameter (m)	D_r	3.5	
	transmission	τ_r	0.5	
Corner cube parameters	cube diameter (cm)	d_{cube}	3.8	
	divergence angle (μ rad)	θ_{cube}	42	
	reflection efficiency	τ_{cube}	0.245	
	number of elements--Apollo 11, Apollo 14 (used in report). (Apollo 15)	n_{cube}	100 (300)	

* Uses guide star adaptive optics performance simulations

B. Ellerbroek, AF Phillips Laboratory, Albuquerque, NM

CEMERLL Intensity fluctuations

Expected photon returns:

- Product of initial laser strength, propagation and transmission factors

$$i = \eta_{uplink} \eta_{cubes} \eta_{downlink}$$

$$\eta_{uplink} = \left(\frac{\lambda p}{hc} \times \tau_{tr} \right) \times \tau_{atm} \times \left(\frac{\frac{\pi D_{tr}^2}{4}}{(\lambda range)^2} \right) i_{rel}$$

$$\eta_{cubes} = N_{cube} \left(\frac{\pi d_{cube}^2}{4} \right) \times \tau_{cube}$$

$$\eta_{receiver} = \tau_{atm} \times \left(\frac{D_r}{\theta_{cube} range} \right)^2 \times \tau_r$$

CEMERLL Intensity fluctuations

Expected photon returns (2):

Condition	$\lambda=532$ nm	$\lambda=1064$ nm	beam quality
uncompensated	12	9s	broad speckle pattern of low intensity
compensated	17	155	concentrated beam with uncorrected atmospheric tilt
compensated +tilt corrected	304	5,240	well localized beam; objective for extended CEMERLL experiment
maximum	5,687	12,300	maximum for perfect adaptive optics

CEMERLL Intensity fluctuations

Uplink pdf theory:

- random walk model for intensity partitioned into specular and diffuse components:

specular component corresponds to unperturbed portion of beam

diffuse component corresponds to scattered portion of beam

higher order turbulence, focal anisoplanatism

- on-axis complex amplitude model:

$$\begin{aligned} a(0,0) &= a_s(0,0) + a_d(0,0) \\ a(0,0) &= \sum_{k=1}^K a_{sk}(0,0) e^{i\psi_k(0,0)} + \sum_{k=1}^K a_{dk}(0,0) e^{i\phi_k(0,0)} \end{aligned}$$

resultant intensity:

$$i = |a(0,0)|^2$$

- K becomes α as continuous parameter for effective number of scattering elements

CEMERLL Intensity fluctuations

Uncompensated uplink pdf:

■ I-K distribution based on Andrews and Phillips model

assumes infinite number of diffuse scatterers:

$$p(i_u) = \begin{cases} \frac{2\alpha}{b} \left(\frac{\sqrt{i_u}}{A} \right)^{\alpha-1} K_{\alpha-1} \left(2A \sqrt{\frac{\alpha}{b}} \right) I_{\alpha-1} \left(2 \sqrt{\alpha \frac{i_u}{b}} \right) & (i_u < A^2) \\ \frac{2\alpha}{b} \left(\frac{\sqrt{i_u}}{A} \right)^{\alpha-1} I_{\alpha-1} \left(2A \sqrt{\frac{\alpha}{b}} \right) K_{\alpha-1} \left(2 \sqrt{\alpha \frac{i_u}{b}} \right) & (i_u > A^2) \end{cases}$$

pdf can approach lognormal pdf for weak turbulence or exponential pdf for strong turbulence

■ moments and parameters:

$$\langle i_u^n \rangle = \left(\frac{b}{\alpha} \right)^n n! \sum_{k=0}^n \frac{\Gamma(\alpha+n) (\alpha\rho)^k}{\Gamma(\alpha+k) k!} \quad \rho = \frac{A^2}{b}$$

$$\langle i_u \rangle = A^2 + b$$

$$\langle i_u^2 \rangle = A^4 + 2A^2b + 2b^2 + \frac{2}{\alpha} b (b + A^2)$$

CEMERLL Intensity fluctuations

Relation of parameters to intensity moments and experimental conditions:

- Coherence area: $\alpha = \frac{A_{beam}}{A_c}$

$$A_c \approx \int_{-\infty}^{\infty} \int |\mu(\Delta x, \Delta y)|^2 d\Delta x d\Delta y = 2\pi \int_0^{\frac{D_{tr}}{2}} r e^{-6.88 \left(\frac{r}{r_0}\right)^{5/3}} dr$$

$$\alpha = 2.3 \left(\frac{D}{r_0}\right)^2$$

- Far-field diffraction integral:

$$\langle I(0, 0) \rangle = \frac{I_0}{(\lambda z)^2} \int \int \int \int_D \mu(\xi, \eta, \xi', \eta') d\xi d\eta d\xi' d\eta' = \frac{I_0}{(\lambda z)^2} \int \int \int \int_D e^{-3.44 \left(\frac{(\xi - \xi')^2 + (\eta - \eta')^2}{r_0^2} \right)^{5/6}} d\xi d\eta d\xi' d\eta'$$

- Compare to diffraction limit:

$$i_{turb} = \frac{\langle I(0, 0) \rangle_{dl}}{\langle I(0, 0) \rangle} = \left(\frac{r_0}{D}\right)^2$$

$$\langle i_i \rangle = \left(\frac{\lambda p}{hc} \times \tau_{atm}\right) \times \tau_{tr} \times \left[\frac{\frac{\pi D_{tr}^2}{4}}{(\lambda \times range)^2} \right] \times i_{turb}$$

CEMERLL Intensity fluctuations

Approximation for second moment:

■ limiting case for large α and small ρ

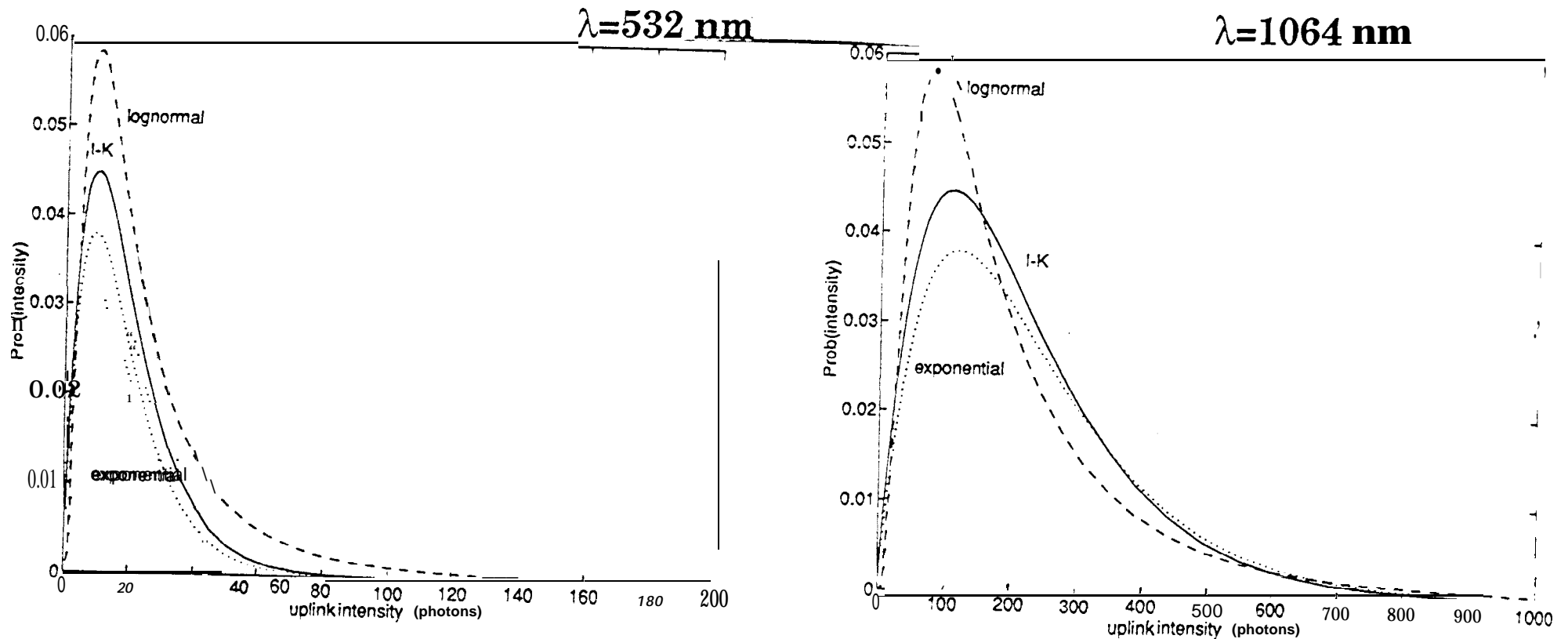
$$\langle i_u^2 \rangle = 2(1 + \dots) \langle i_u \rangle^2$$

CEMERLL Intensity fluctuations

Uncompensated uplink prediction:

λ	r_0	α	$\langle i_u \rangle$ (photons)	$\langle i_u^2 \rangle / \langle i_u \rangle^2$	A^2 (photons)	b (photons)
532 nm	7 cm	1379	9.5	2.0015	7.1×10^{-12}	9.5
1064 nm	7 cm	261.9	108.2	2.0076	1 0 ⁸	108.2

■ Probability density for $r = 7$ cm



CEMERLL Intensity fluctuations

Compensated pdf:

■ Assumption on random walk model:

small number of scatterers

specular component jitters due to uncompensated atmospheric tilt

diffuse component due to uncorrected aberrations (e.g. focal anisoplanatism or limited AO corrections)

final pdf is integral of unlittered pdf and jitter pdf

■ Unlittered pdf is Nakagami distributed:

$$p(i_c | i_s) = \frac{\alpha}{b} \left(\frac{\sqrt{i_c}}{\sqrt{i_s}} \right)^{\alpha-1} e^{-\alpha \frac{(A^2 i_s + i_c)}{b}} I_{\alpha-1} \left(2\alpha \frac{A}{b} \sqrt{i_c i_s} \right)$$

■ Jitter pdf (Kiasaleh and Yan):

$$p(i_s) = \beta i_s^{\beta-1} \quad 0 \leq i_s \leq 1$$

$$\langle (i_c | i_s) \rangle = A^2 i_s + b$$

$$\langle i_c \rangle = A^2 \left(\frac{\beta}{1+\beta} \right) + b$$

CEMERLL Intensity fluctuations

Relating intensity moments to experimental conditions:

■ jitter parameters

$$\beta = \frac{\left(\frac{\lambda}{2D_{tr}}\right)^2}{\sigma_j^2}$$

$$\sigma_j^2 = 0.1812\left(\frac{\lambda}{D_{tr}}\right)^{1/3}\left(\frac{\lambda}{r_0}\right)^{5/3} + (0.6\mu rad)^2$$

■ Solve for parameters:

$$A^2 = \frac{\langle\langle i_c | i_s \equiv 1 \rangle\rangle - \langle i_c \rangle}{1 - \beta}$$

$$b = -\frac{\left(\langle i_c \rangle - \beta \langle\langle i_c | i_s \equiv 1 \rangle\rangle\right)}{1 - \beta}$$

■ Approximate r. provides approximation for α

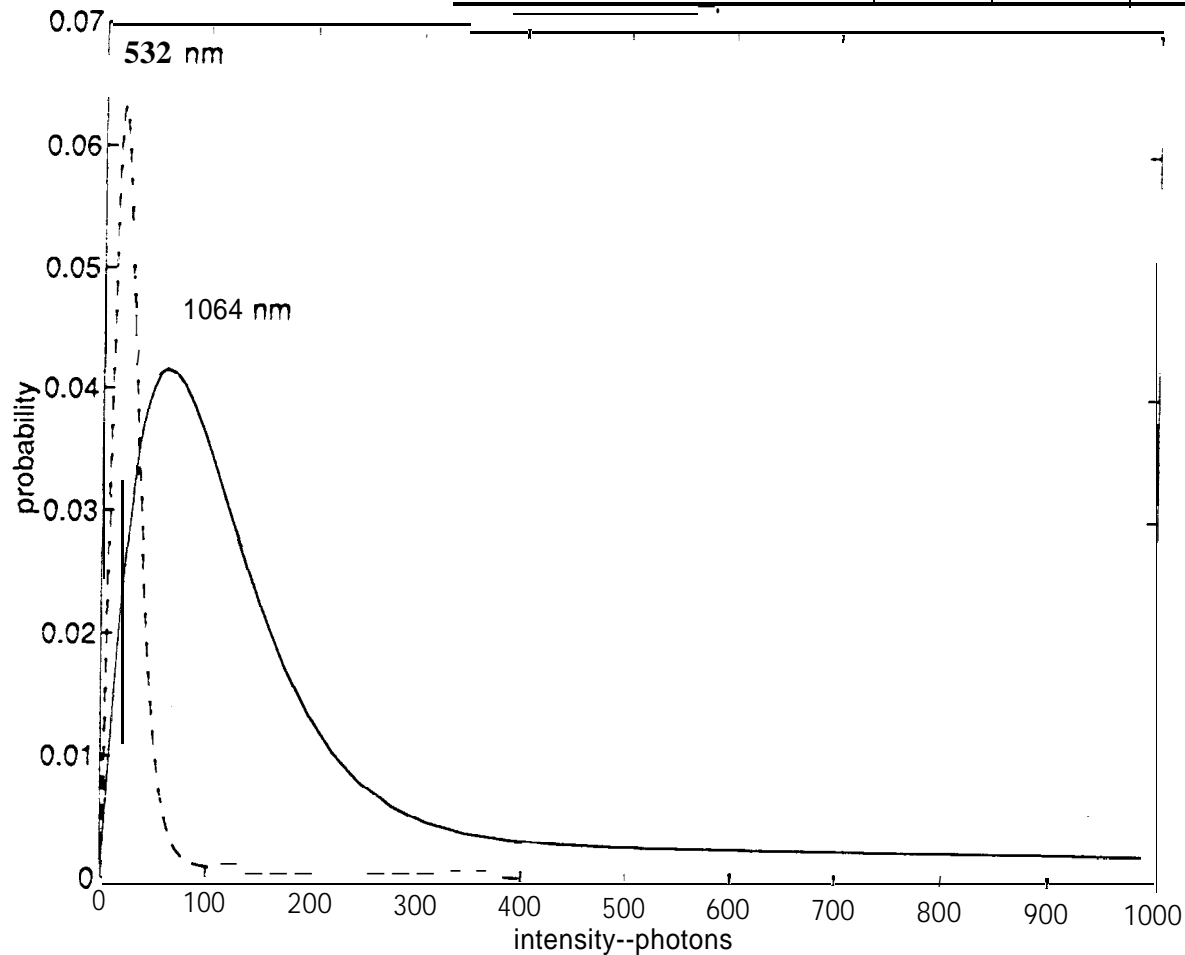
$$O_{eq} = \frac{4\lambda}{\pi\theta_{seeing}} \quad \theta_{seeing} = 0.13 \text{ arc sec}$$

■ mean intensities from laser guidestar simulated performance

CEMERLL Intensity fluctuations

Predicted compensated uplink pdf:

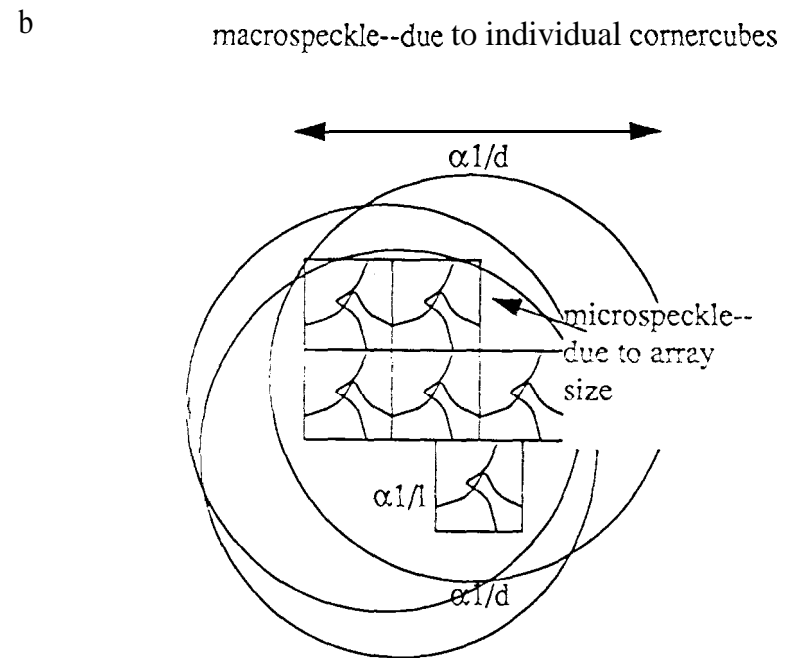
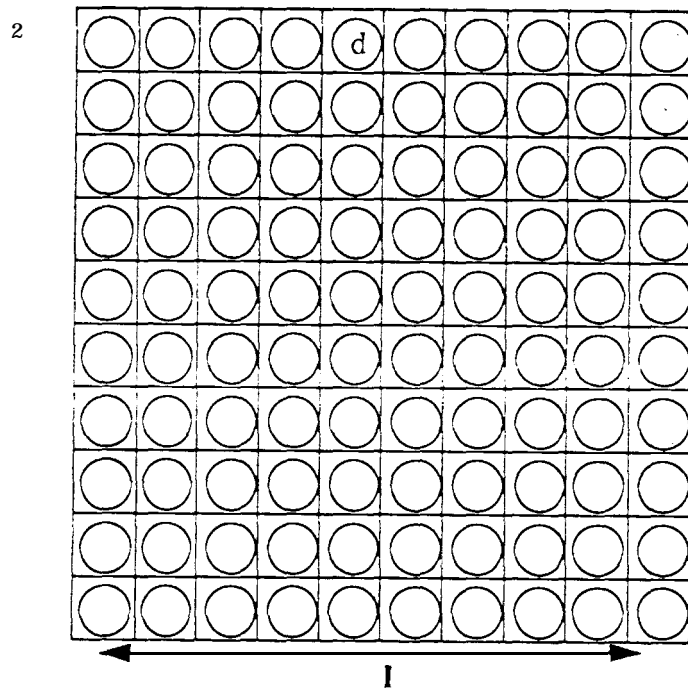
wavelength	effective r.	α	jittered intensity $\langle i_c \rangle$ (photons)	tilt corrected intensity $\langle i_c i_s = 1 \rangle$ (photons)	a	β	A^2 (photons)	b (photons)
532 nm	1.67 m	2.36	21	464	2.363	0.00621	446.3	17.7
1064 nm	3.84 m	1.27	214	6505	1.270	0.02498	6451	54



CEMERLL Intensity fluctuations

Properties of retroreflected beam:

- Incoherent array of radiators causes a fixed, unknown speckle pattern of microspeckle and macro speckle



- **Beam** coherence diameter at top of atmosphere is 600 **mat** 532 nm and 1200 m at 1064 nm
- **Retroreflected beam is a modulated plane wave at top of the atmosphere**
modulation is due to uplink variations

CEMERLL Intensity fluctuations

Downlink beam breakup:

- Assumes random walk model

log normal intensity pdf for weak turbulence

exponential pdf for strong turbulence

- Detection by large aperture receiver

Detected intensity averages all downlink fluctuations

$$E = \frac{A_r}{N} \sum_{j=1}^J \sum_{k=1}^K I(x_j, y_k) \quad N = J \times K = 2.3 \left(\frac{D_r}{r_0} \right)^2$$

$$\sigma_E^2 = \frac{A^2 \sigma_I^2}{N}$$

- Downlink integrated intensity fluctuations are insignificant compared to uplink fluctuations
- Two way link intensity pdf dominated by uplink pdf

CEMERLL Intensity fluctuations

Signal detection:

- Candidate detectors, PMT, SSPM, APD, are all photovoltaic
- Analog detection required due to short laser pulse duration

output Current proportional to input signal, detector quantum efficiency and gain
signal fluctuations quantified by production of secondary photoelectrons

$$n_s = G \times (n_p + n_{back})$$

assume Poisson dark noise can be corrected

- pdf for primary photoelectrons is Poisson (Mandel) transform of integrated intensity:

$$p(n_p) = \int_0^{\infty} \frac{W^n e^{-W}}{n_p!} p(W) dW$$
$$W = qe \times E$$

- PMT and SSPM gain fluctuations do not smear $p(n_s)$

CEMERLL Intensity fluctuations

Secondary photoelectron pdf's under APD gain fluctuations:

- $$p(TZJ) = \sum_{n_p} p(n_p, n_s; G) \times p(n_p)$$

- From McIntyre (RCA Review, 1972)**

$$p(n_p, n_s = n_p + r; G) = \frac{n_p (1-k)^r \Gamma\left(\frac{n_p + r}{1-k}\right)}{(n_p + kr)^r \Gamma\left(\frac{n_p + kr}{1-k}\right)} \left(\frac{1 + k(G-1)}{G}\right)^{\frac{(n_p + kr)}{(1-k)}} \left(\frac{G-1}{G}\right)^r$$

- APD gain fluctuations influence pdf tails**

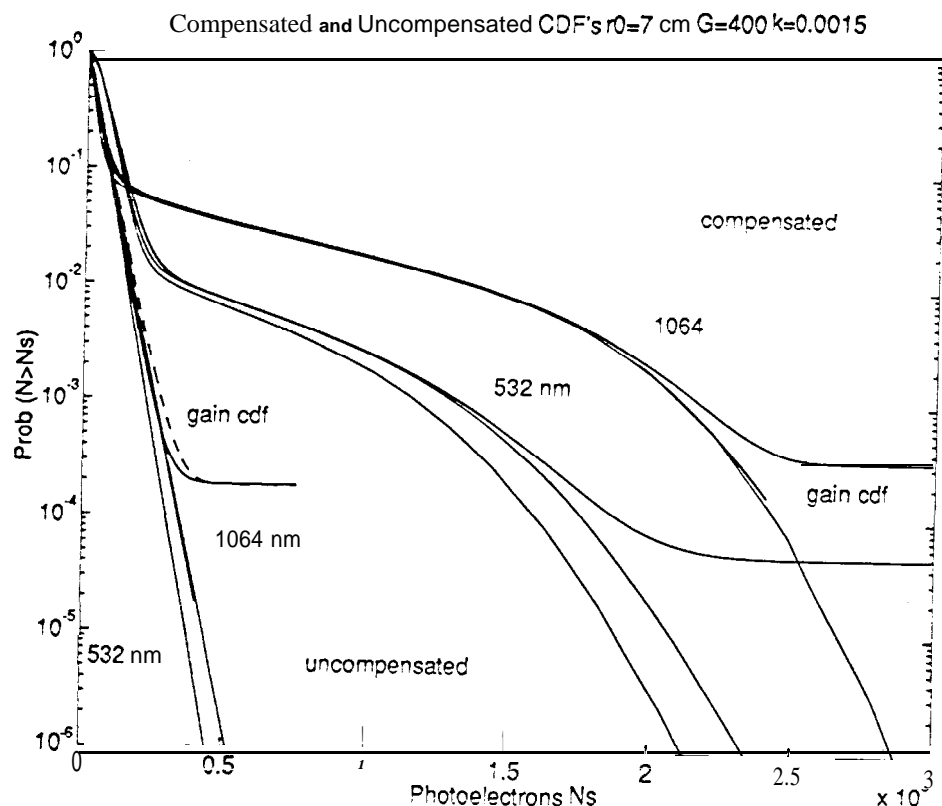
CEMERLL Intensity fluctuations

Primary photoelectron calfs:

- Comparison of $p(n_s)$, $G \times p(n_p)$ and $G \times p(qe \times W)$

- $\text{Calf}(n) = \sum_{k=n}^{\infty} p(n)$

$qe = 80\%$ at 532 nm and 8% at 1064 nm



- Average photons levels do not significantly change pdf's

CEMERLL Intensity fluctuations

Summary:

- Computed expected signal levels for CEMERLL
 - Derived pdf for compensated and uncompensated uplink fo CEMERLL
- Related parameters of pdf's to experimental conditions
- Uplink fluctuations dominate over cornercube reflection, downlink propagation through atmosphere, and aperture averaging from receiver
 - Expected signal changes slightly with detection and with gain variation

CEMERLL Intensity fluctuations

Acknowledgments:

- Brent Ellerbroek-- USAF Phillips Laboratory
- Keith Wilson, Tsun-Yee Yan, and Jim Lesh--JPL Optical Communications Group
- Mike Shao--JPL Interferometry Group